# Compressed sensing in photoacoustic tomography with in vivo experiments

Zijian Guo, Changhui Li, Liang Song, Lihong V. Wang

Zijian Guo, Changhui Li, Liang Song, Lihong V. Wang, "Compressed sensing in photoacoustic tomography with in vivo experiments," Proc. SPIE 7564, Photons Plus Ultrasound: Imaging and Sensing 2010, 75640J (11 February 2010); doi: 10.1117/12.841311

SPIE.

Event: SPIE BiOS, 2010, San Francisco, California, United States

# Compressed sensing in photoacoustic tomography with *in vivo* experiments

Zijian Guo, Changhui Li, Liang Song, and Lihong V. Wang*

Optical Imaging Laboratory, Department of Biomedical Engineering, Washington University
1 Brookings Drive, Saint Louis, Missouri 63130, USA

## ABSTRACT

The data acquisition speed in photoacoustic computed tomography (PACT) is limited by the laser repetition rate and the number of parallel ultrasound detecting channels. Reconstructing PACT image with a less number of measurements can effectively accelerate the data acquisition and reduce the system cost. Recently emerged Compressed Sensing (CS) theory enables us to reconstruct a compressible image with a small number of projections. This paper adopts the CS theory for reconstruction in PACT. The idea is implemented as a non-linear conjugate gradient descent algorithm and tested with phantom and *in vivo* experiments.

**Keywords:** Photoacoustic imaging, compressed sensing

## 1. INTRODUCTION

The field of photoacoustic tomography (PAT) has been expanding rapidly in the past few years [1]. By combining strong optical absorption contrast and high ultrasonic resolution in a single modality, PAT can achieve much better spatial resolution at depths beyond the optical ballistic regime (~1 mm in the skin) than the traditional optical modalities [2, 3]. In PAT, biological tissues are usually irradiated by a pulsed laser. Absorbed energy is converted into heat, which is further converted to a pressure rise via thermoelastic expansion. The initial pressure rise then propagates as ultrasonic waves, which are detected by ultrasound sensors, and the received ultrasonic signals are used to form an image. When the excitation laser is replaced by microwave or RF sources, the technique is called thermoacoustic tomography (TAT) [4, 5]. Both PAT and TAT have been used successfully in a variety of applications, including high-quality *in vivo* vascular structural imaging, hemodynamic functional imaging [6, 7], visualization of breast tumors [8, 9], and molecular imaging of biomarkers with exogenous contrast agents [10-12].

PAT has been implemented in various forms, and each form has its own advantages and applications [1]. In this paper, we focus on photoacoustic computed tomography (PACT, or simply PAT), in which an array of unfocused ultrasonic transducers is placed outside the object, and an inverse algorithm is used to reconstruct the image. Closed form reconstruction formulas have been reported in both the frequency and time domains for spherical, planar, and cylindrical detecting geometries [13-20]. However, a fundamental assumption of all these algorithms is that the spatial sampling of the detecting aperture is sufficient; otherwise, undersampling artifacts, such streaking artifacts or grating lobes, appear.

Reliable image reconstruction with sparse sampling of the detecting aperture is desirable. In practical PAT systems, it is recommended [1, 21] to set the discrete spatial sampling period to be two to five times smaller than the sensing aperture of the detector. For a scanning PAT system, it may require hundreds or even thousands of scanning steps to acquire an image, depending on the sizes of both the detector and the detecting aperture. Such scanning usually takes several minutes to complete. To reach real-time imaging, PAT is implemented with an array of ultrasonic transducers, where all or groups of the array elements can detect photoacoustic signals simultaneously. However, the data acquisition speed is still limited by the number of parallel data acquisition (DAQ) channels, and employing a large number of DAQ channels greatly increases the system cost. For example, for a fast 512-element

* Corresponding author. Email: lhwang@biomed.wustl.edu

Photons Plus Ultrasound: Imaging and Sensing 2010, edited by Alexander A. Oraevsky, Lihong V. Wang,
Proc. of SPIE Vol. 7564, 75640J · © 2010 SPIE · CCC code: 1605-7422/10/$18 · doi: 10.1117/12.841311

ring array PAT system with a 64 channel data acquisition module [22], it takes 8 laser shots to collect data from all 512 elements. For direct 3-D reconstruction PAT applications [23, 24], the data from a 2-D ultrasonic array is usually an extremely sparse sampling of the detecting aperture. Moreover, channel crosstalk is also related to the space between neighboring elements (kerf), and an extensive spatial sampling may increase the crosstalk.

Imaging an object in PAT can be understood as sensing the object in a certain domain. For example, with the 'Fourier-shell identity' [25], PAT can be seen as detecting the spatial frequencies of the object (sensing in the Fourier domain). Sparse spatial sampling of the detecting aperture implies that only partial spatial frequency components can be detected. Traditional backprojection (BP) reconstruction methods [16] simply assume those unobserved frequencies to be zeros. According to Parseval's theorem, the BP method reconstructs the image of "minimal energy" under the observation constraints. An improved reconstruction algorithm should be able to "guess" these unobserved frequency components. However, interpolation in the Fourier domain is a critical issue, and usually creates artifacts in reconstructed images [26]. The recently developed compressed sensing (CS) theory [27] enables us to recover these unobserved components under certain conditions. The theory has been successfully applied in MRI [28], where MRI images were able to be reconstructed from significantly undersampled K-space measurements. Paper [29] first introduced the CS theory into the field of PAT, and the idea was tested with phantoms from a circular scanning PAT system. In this paper, we improve the speed of the reconstruction algorithm by adopting a non-linear conjugate gradient descent method. Also, we demonstrate the algorithm with both phantom and animal data, using various detecting geometries.

## 2. METHODS

The CS theory was rigorously formulated to reconstruct images from incomplete datasets. To make this possible, the CS theory relies on two principles: sparsity, which pertains to the object of interest, and incoherence, which pertains to the sensing modality. A non-linear reconstruction is used to enforce both sparsity of the image representation and consistency with the acquired data. Unlike ultrasound imaging and all other coherent imaging technologies, PAT is devoid of speckle artifacts and sensitive to boundaries because of its optical absorption contrast [30]. Therefore, computing the Finite Difference (FD) of PAT images in the spatial domain sometimes directly results in a sparse representation. When imaging complex absorbing structures such as the blood vessels in the mouse brain cortex, however, PAT images may not be sparse in the spatial domain. In these cases, we need to project the images onto an appropriate basis set, such as the wavelet basis. Readers are referred to paper [29] about the discussion on the incoherent condition.

In the CS theory, the reconstruction of image $x$ is obtained by solving the following constrained optimization problem:

$$\min_x \left|\Psi x\right|_1 \text{ s.t. } \left|\Phi x - y\right|_2 < \varepsilon \text{ . (1)}$$

Here $\Psi$ and $\Phi$ are defined as the sparsifying transform matrix and the forward projection matrix, $y$ is the measured data, and $\varepsilon$ is the parameter that controls the fidelity of the reconstruction to $y$. The parameter $\varepsilon$ is usually set based on the expected noise level. The object function in Eq. (1) is the $l_1$ norm (defined as $\left|x\right|_1 = \sum \left|x_i\right|$). The $l_1$ norm is used here instead of the $l_2$ norm (defined as $\left|x\right|_2 = \sqrt{\sum \left|x_i\right|^2}$), because the $l_2$ norm penalizes large coefficients heavily, and leads to non-sparsity. In the $l_1$ norm, many small coefficients tend to carry a much larger penalty than a few large coefficients, therefore small coefficients are suppressed and solutions are often sparse. In Eq. (1), minimizing the $l_1$ norm of $\Psi x$ promotes sparsity, and the constraint enforces data consistency. The algorithm is implemented with a non-linear conjugate gradient descent method [31]. On a laptop with a dual-core 2-GHz CPU and 3-GB memory, the calculations usually take less than 10 minutes using Matlab 2008a.

## 3. RESULTS

### 3. A. Numerical simulation

We first demonstrate the CS method using a numerical phantom simulation with a circular detecting geometry. The simulation can be summarized in four steps:

1) Generate measurements $y$ from a phantom $x$, using the PAT forward operator $\Phi$, by obeying the relation $y = \Phi x$.

2) Add 5% random noise into the generated measurement $y' = y + e$.

3) From the noisy measurement $y'$, reconstruct the image with the BP method $\bar{x} = \Phi^{-1} y'$.

4) Starting with $\bar{x}$ as the initial guess, iteratively solve Eq. (3) with the algorithm presented in the Appendix.

Figure 1 shows a numerical experiment conducted on a 10 mm × 10 mm phantom with a 256 × 256 resolution. The circular detecting radius is set to be 25 mm. All the detectors are assumed to be point detectors, whose detecting angles are assumed to cover the whole FOV. We compare the CS reconstructions with the BP reconstructions. Figure 1 (a) shows the original numerical phantom. The BP reconstruction results with 256, 128, and 64 tomographic angles are shown in Figs. 1 (b), (c), and (d), respectively. The corresponding results with CS reconstruction are shown in Figs. 1 (e), (f), and (g), where the images are reconstructed with the CS method by using the FDWT and the FD together as the sparsifying transforms. We can observe that the CS reconstruction is clearly superior to the BP reconstruction. This can be shown by extracting a line from the original numerical phantom. The interference level has been reduced significantly with the CS reconstruction. Moreover, as predicted by the theory, the CS scheme is robust to inaccurate measurements, so the noise level has also been suppressed.

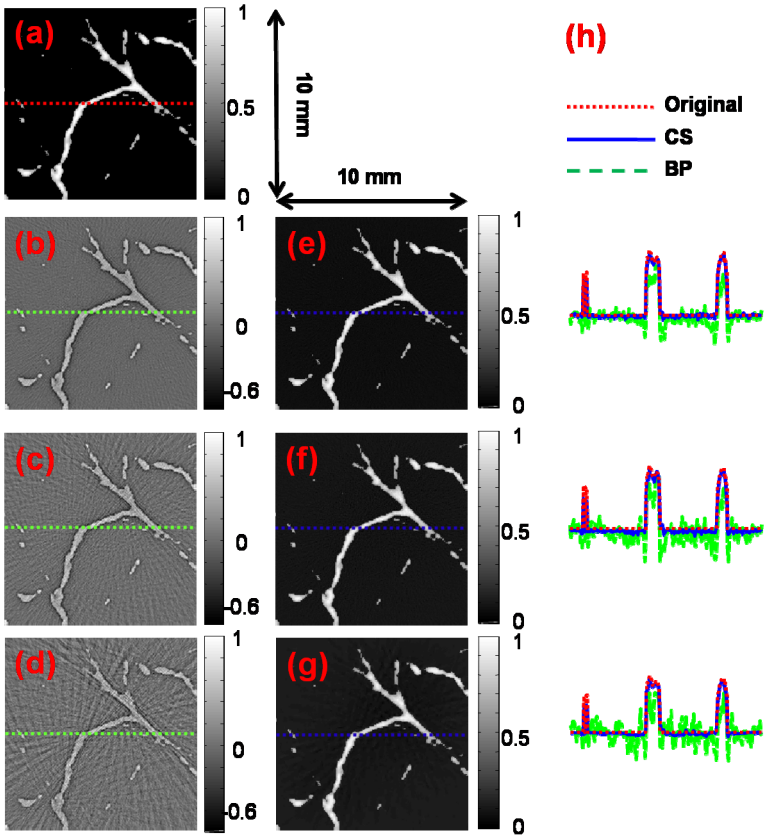

Figure 1 **Numerical simulations.** (a) A 10 mm×10 mm blood-vessel containing phantom with 256×256 pixels; (b), (c), and (d) Images reconstructed using the BP method with 256, 128 and 64 tomographic angles; (e), (f), and (g) Images reconstructed using the CS method with 256, 128 and 64 tomographic angles; (h) Lines extracted from (a-g).

### 3. B. Phantom experiments

Tissue phantoms were imaged by scanning a virtual point detector in a setup similar to that of [32]. The PA source contained three black human hair crosses glued on top of optical fibers, with an interval between the hair crosses of about 10 mm. Laser pulses with a repetition rate of 10 Hz were diverged by a ground glass to achieve a relatively uniform illumination. The virtual point detectors evenly scanned the object along a horizontal circle, stopping at 240 points, and the signals were averaged over 20 times at each stop. The total data acquisition time was 8 minutes. Figure 2 shows the reconstruction results with the BP (a, b), the CS (c, d), and the traditional iterative reconstruction (IR) [33] (e, f) methods, with 240, 120 and 80 tomographic angles. We reconstructed the image with a FOV of 30 mm × 15 mm. As expected, we could reconstruct the phantoms adequately with a small number of detecting positions. The data acquisition time in the circular scanning geometry can be improved by fourfold with the CS reconstruction method.

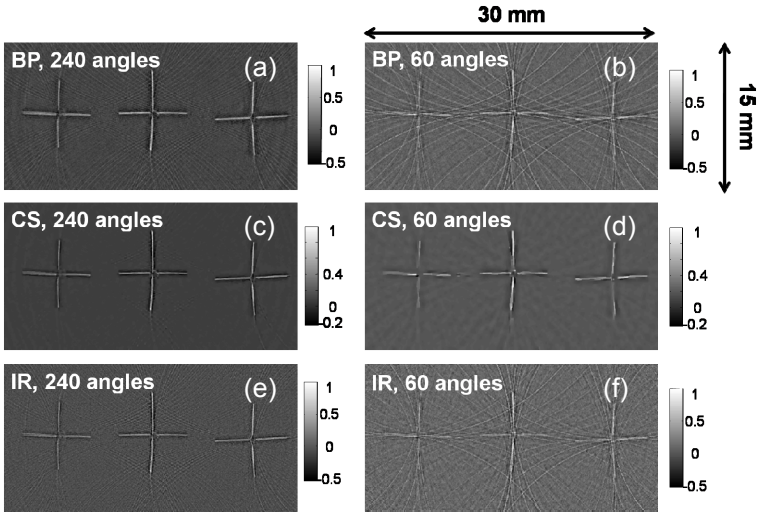


Figure 2 **Tissue phantom imaging with a virtual point detector.** (a), (b) Images reconstructed using the BP method with 240 and 60 tomographic angles; (c), (d) Images reconstructed using the CS method with 240 and 60 tomographic angles; (e), (f) Images reconstructed using the IR method with 240 and 60 tomographic angles

### 3. C. *In vivo* experiments

*In vivo* experiment was based on a custom designed 512-element photoacoustic tomography array system [22]. The 5 MHz piezocomposite transducer array was formed into a complete circular aperture. With a 64-channel data acquisition module, the system could provide full tomographic imaging at up to 8 frames/second. We used this system to image mouse cortical blood vessels. The images were reconstructed by the BP (a, b), the IR (c) and the CS (d) algorithms. As shown in Fig. 3, we could reconstruct the *in vivo* image adequately with a small number of detecting positions.

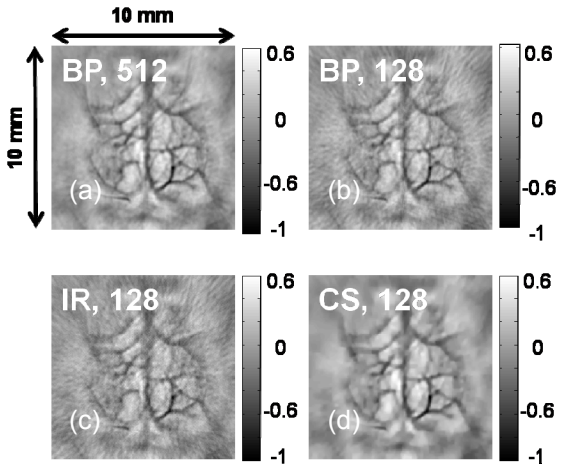


Figure 3 ***In vivo*** **imaging of the mouse cortex with a circular ultrasonic array.** (a), (b) Images reconstructed using the BP method with 512 and 128 detecting elements; (c) Image reconstructed using the IR method with 128 detecting elements; (d) Image reconstructed using the CS method with 128 detecting elements.

## 4. CONCLUSIONS

We have shown how the CS theory can be used for reconstruction in PAT with a limited number of measurements. Both simulation and experimental results show that the CS method can effectively reduce the undersampling artifacts. By incorporating the CS theory in the PAT reconstruction, we can effectively reduce the system cost, or cover a larger FOV with the same number of measurements. Although the CS method is only demonstrated here with 2D problems, the generalization to 3D reconstructions is straight forward.

## ACKNOWLEDGMENTS

This work was sponsored in part by National Institutes of Health grants R01 EB008085, U54 CA136398, R01 CA113453901, R01 NS46214 (BRP) and R01 EB000712. L. W. has a financial interest in microphotoacoustic, Inc. and Endra, Inc., which, however, did not support this work.

## REFERENCES

[1] Xu, M. H.,Wang, L. H. V., "Photoacoustic imaging in biomedicine," *Review of Scientific Instruments,* 77 (4), -, (2006).

[2] Wang, L. V.,Wu, H., [*Biomedical Optics: Principles and Imaging*] Wiley: Hoboken, NJ, (2007).

[3] Wang, L. V., "Tutorial on photoacoustic microscopy and computed tomography," *Ieee Journal of Selected Topics in Quantum Electronics,* 14 (1), 171-179, (2008).

[4] Kruger, R. A., Reinecke, D. R.,Kruger, G. A., "Thermoacoustic computed tomography–technical considerations," *Medical Physics,* 26 (9), 1832-1837, (1999).

[5] Wang, L. H. V., Zhao, X., Sun, H.,Ku, G., "Microwave-induced acoustic imaging of biological tissues," *Review of Scientific Instruments,* 70 (9), 3744-3748, (1999).

[6] Wang, X. D., Pang, Y. J., Ku, G., Xie, X. Y., Stoica, G.,Wang, L. H. V., "Noninvasive laser-induced photoacoustic tomography for structural and functional in vivo imaging of the brain," *Nature Biotechnology,* 21 (7), 803-806, (2003).

[7] Zhang, H. F., Maslov, K., Stoica, G.,Wang, L. H. V., "Functional photoacoustic microscopy for high-resolution and noninvasive in vivo imaging," *Nature Biotechnology,* 24 (7), 848-851, (2006).

[8] Kruger, R. A., Reynolds, H. E., Kiser, W., Reinecke, D. R.,Kruger, G. A., "Thermoacoustic computed tomography for breast imaging," *Radiology,* 210 (2), 587-587, (1999).

[9] Oraevsky, A. A., Savateeva, E. V., Solomatin, S. V., Karabutov, A. A., Andreev, V. G., Gatalica, Z., Khamapirad, T.,Henrichs, P. M., Optoacoustic imaging of blood for visualization and diagnostics of breast cancer. In *Proc. SPIE*, 2002; Vol. 4618, pp 81-94.
[10] Li, L., Zemp, R. J., Lungu, G., Stoica, G.,Wang, L. H. V., "Photoacoustic imaging of lacZ gene expression in vivo," *Journal of Biomedical Optics,* 12 (2), -, (2007).
[11] Li, M. L., Oh, J. T., Xie, X. Y., Ku, G., Wang, W., Li, C., Lungu, G., Stoica, G.,Wang, L. V., "Simultaneous molecular and hypoxia imaging of brain tumors in vivo using spectroscopic photoacoustic tomography," *Proceedings of the Ieee,* 96 (3), 481-489, (2008).
[12] De La Zerda, A., Zavaleta, C., Keren, S., Vaithilingam, S., Bodapati, S., Liu, Z., Levi, J., Smith, B. R., Ma, T. J., Oralkan, O., Cheng, Z., Chen, X. Y., Dai, H. J., Khuri-Yakub, B. T.,Gambhir, S. S., "Carbon nanotubes as photoacoustic molecular imaging agents in living mice," *Nature Nanotechnology,* 3 (9), 557-562, (2008).
[13] Xu, Y., Feng, D. Z.,Wang, L. H. V., "Exact frequency-domain reconstruction for thermoacoustic tomography - I: Planar geometry," *Ieee Transactions on Medical Imaging,* 21 (7), 823-828, (2002).
[14] Xu, Y., Xu, M. H.,Wang, L. H. V., "Exact frequency-domain reconstruction for thermoacoustic tomography - II: Cylindrical geometry," *Ieee Transactions on Medical Imaging,* 21 (7), 829-833, (2002).
[15] Xu, M. H., Xu, Y.,Wang, L. H. V., "Time-domain reconstruction-algorithms and numerical simulations for thermoacoustic tomography in various geometries," *Ieee Transactions on Biomedical Engineering,* 50 (9), 1086-1099, (2003).
[16] Xu, M. H.,Wang, L. V., "Universal back-projection algorithm for photoacoustic computed tomography (vol 71, art no 016706, 2005)," *Physical Review E,* 75 (5), -, (2005).
[17] Finch, D., Patch, S. K.,Rakesh, "Determining a function from its mean values over a family of spheres," *SIAM J. Math. Anal.,* 35 (5), 1213-1240, (2004).
[18] Kruger, R. A., Liu, P. Y., Fang, Y. R.,Appledorn, C. R., "Photoacoustic Ultrasound (Paus) - Reconstruction Tomography," *Medical Physics,* 22 (10), 1605-1609, (1995).
[19] Kostli, K. P., Frenz, M., Bebie, H.,Weber, H. P., "Temporal backward projection of optoacoustic pressure transients using Fourier transform methods," *Physics in Medicine and Biology,* 46 (7), 1863-1872, (2001).
[20] Hoelen, C. G. A., de Mul, F. F. M., Pongers, R.,Dekker, A., "Three-dimensional photoacoustic imaging of blood vessels in tissue," *Optics Letters,* 23 (8), 648-650, (1998).
[21] Cox, B. T., Arridge, S. R.,Beard, P. C., "Photoacoustic tomography with a limited-aperture planar sensor and a reverberant cavity," *Inverse Problems,* 23 (6), S95-S112, (2007).
[22] Gamelin, J., Maurudis, A., Aguirre, A., Huang, F., Guo, P., Wang, L. V.,Zhu, Q., "A real-time photoacoustic tomography system for small animals " *Opt. Express,* 17 (13), 10489-10498, (2009).
[23] Ephrat, P., Roumeliotis, M., Prato, F. S.,Carson, J. J. L., "Four-dimensional photoacoustic imaging of moving targets," *Optics Express,* 16 (26), 21570-21581, (2008).
[24] Ephrat, P., Keenliside, L., Seabrook, A., Prato, F. S.,Carson, J. J. L., "Three-dimensional photoacoustic imaging by sparsearray detection and iterative image reconstruction," *Journal of Biomedical Optics,* 13 (5), -, (2008).
[25] Anastasio, M. A., Zhang, J., Modgil, D.,La Riviere, P. J., "Application of inverse source concepts to photoacoustic tomography," *Inverse Problems,* 23 (6), S21-S35, (2007).
[26] Haltmeier, M., Zangerl, G.,Scherzer, O., A Reconstruction Algorithm for Photoacoustic Imaging based on the Nonuniform FFT. In *Research Network FWF S105: Photoacoustic Imaging in Medicine and Biology*, 2008.
[27] Candes, E. J., Romberg, J.,Tao, T., "Robust uncertainty principles: Exact signal reconstruction from highly incomplete frequency information," *Ieee Transactions on Information Theory,* 52 (2), 489-509, (2006).
[28] Lustig, M., Donoho, D.,Pauly, J. M., "Sparse MRI: The application of compressed sensing for rapid MR imaging," *Magnetic Resonance in Medicine,* 58 (6), 1182-1195, (2007).
[29] Provost, J.,Lesage, F., "The Application of Compressed Sensing for Photo-Acoustic Tomography," *Ieee Transactions on Medical Imaging,* 28 (4), 585-594, (2009).
[30] Guo, Z., Li, L.,Wang, L. V., "On the speckle-free nature of photoacoustic tomography," *Medical Physics,* 36 (9), (2009).
[31] Figueiredo, M. A. T., Nowak, R. D.,Wright, S. J., "Gradient Projection for Sparse Reconstruction: Application to Compressed Sensing and Other Inverse Problems," *Ieee Journal of Selected Topics in Signal Processing,* 1 (4), 586-597, (2007).
[32] Li, C. H.,Wang, L. V., "High-numerical-aperture-based virtual point detectors for photoacoustic tomography," *Applied Physics Letters,* 93 (3), -, (2008).
[33] Paltauf, G., Viator, J. A., Prahl, S. A.,Jacques, S. L., "Iterative reconstruction algorithm for optoacoustic imaging," *Journal of the Acoustical Society of America,* 112 (4), 1536-1544, (2002).